Stanford Exploration Project, Report 105, September 5, 2000, pages 157–176

Stanford Exploration Project, Report 105, September 5, 2000, pages 157–176

Multi-dimensional Fourier transforms in the helical coordinate system

James Rickett and Antoine Guitton[1]

ABSTRACT

For every two-dimensional system with helical boundary conditions, there is an isomorphic one-dimensional system. Therefore, the one-dimensional FFT of a 2-D function wrapped on a helix is equivalent to a 2-D FFT. We show that the Fourier dual of helical boundary conditions is helical boundary conditions but with axes transposed, and we explicitly link the wavenumber vector, $\mathbf{k}$, in a multi-dimensional system with the wavenumber of a helical 1-D FFT, k_h. We illustrated the concepts with an example of multi-dimensional multiple prediction.

INTRODUCTION

If helical boundary conditions (Claerbout, 1998b) are imposed on a multi-dimensional system, an isomorphism exists between that system and an equivalent one-dimensional system. Previous authors, for example Claerbout (1998a), take advantage of this isomorphism to perform rapid multi-dimensional inverse filtering by recursion.

The Fourier analogue of convolution is multiplication: to convolve a 2-D signal with a 2-D filter, take their 2-D Fourier transforms, multiply them together and return to the original domain. The relationship between 1-D and 2-D convolution, FFT's and the helix is illustrated in Figure 1. With helical boundary conditions, we can take advantage of the isomorphism described above, and perform multi-dimensional convolutions by wrapping multi-dimensional signals and filters onto a helix, taking their 1-D FFT's, multiplying them together, and then returning to the original domain.

If we can use 1-D FFT's to do 2-D convolutions, the isomorphism due to the helical boundary conditions must extend into the Fourier domain. In this paper, we explore the relationship between 1-D and multi-dimensional FFT's in helical coordinate systems. Specifically we demonstrate the link between the wavenumber vector, $\mathbf{k}$, in a multi-dimensional system, and the wavenumber of a helical 1-D FFT, k_h.

[1]**email:** james@sep.stanford.edu, antoine@sep.stanford.edu

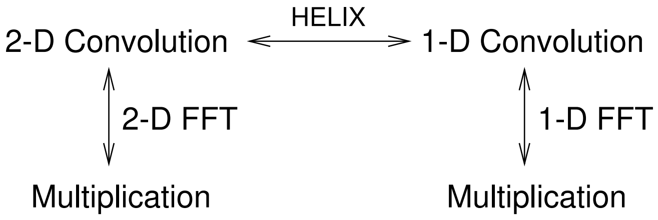

Figure 1: Relationship between 1-D and 2-D convolution, FFT's and the helical boundary conditions. james1-ill [NR]

THEORY

For simplicity, throughout this section we refer to a two-dimensional sampled image, **b**; however, the beauty of the helical coordinate system is that everything can be trivially extended to an arbitrary number of dimensions.

We employ two equivalent subscripting schemes for referring to an element of the two-dimensional image, **b**. Firstly, with two subscripts, b_{p_x,p_y} refers to the element that lies p_x increments along the x-axis, and p_y increments along the y-axis. Ranges of p_x and p_y are given by $0 \leq p_x < N_x$, and $0 \leq p_y < N_y$ respectively. Helical coordinates suggest an alternative subscripting scheme: We can use a single subscript, $p_h = p_x + p_y N_x$, such that $b_{p_x,p_y} = b_{p_h}$ and the range of p_h is given by $0 \leq p_h < N_x N_y$. Moreover, if we impose helical boundary conditions, we can treat **b** as a one-dimensional function of subscript p_h.

Linking 1-D and 2-D FFT's

Taking the one-dimensional Z transform of **b** in the helical coordinate system gives

$$B(Z_h) = \sum_{p_h=0}^{N_x N_y - 1} b_{p_h} Z_h^{p_h}. \tag{1}$$

Here, Z_h represents the unit delay operator in the sampled (helical) coordinate system. The summation in equation (1) can be split into two components,

$$\begin{aligned} B(Z_h) &= \sum_{p_y=0}^{N_y-1} \sum_{p_x=0}^{N_x-1} b_{p_x,p_y} Z_h^{p_x + p_y N_x} & (2) \\ &= \sum_{p_y=0}^{N_y-1} \sum_{p_x=0}^{N_x-1} b_{p_x,p_y}\, Z_h^{p_x}\, Z_h^{N_x p_y}. & (3) \end{aligned}$$

Ignoring boundary effects, a single unit delay in the helical coordinate system is equivalent to a single unit delay on the x-axis; similarly, but irrespective of boundary conditions, N_x unit delays in the helical coordinate system are equivalent to a single delay on the y-axis. This leads to the following definitions of Z_h and $Z_h^{N_x}$ in terms of delay operators, Z_x and Z_y, or wavenumbers, k_x and k_y:

$$\begin{aligned} Z_h &\approx Z_x = e^{ik_x \Delta x}, & (4) \\ Z_h^{N_x} &= Z_y = e^{ik_y \Delta y}, & (5) \end{aligned}$$

where Δx and Δy define the grid-spacings along the x and y-axis respectively.

Substituting equations (4) and (5) into equation (3) leaves

$$B(k_x,k_y) \;=\; B(Z_h) \;=\; \sum_{p_y=0}^{N_y-1}\sum_{p_x=0}^{N_x-1} b_{p_x,p_y}\, Z_x^{p_x}\, Z_y^{p_y} \tag{6}$$

$$= \sum_{p_y=0}^{N_y-1}\sum_{p_x=0}^{N_x-1} b_{p_x,p_y}\, e^{ik_x\Delta x p_x}\, e^{ik_y\Delta y p_y}. \tag{7}$$

Equation (7) implies that, if we ignore boundary effects, the one-dimensional FFT of $\mathbf{b}(x,y)$ in helical coordinates is equivalent to its two-dimensional Fourier transform.

Wavenumber in helical coordinates

With the understanding that the 1-D FFT of a multi-dimensional signal in helical coordinates is equivalent to the 2-D FFT, a natural question to ask is: how does the helical wavenumber, k_h, relate to spatial wavenumbers, k_x and k_y?

The helical delay operator, Z_h, is related to k_h through the equation,

$$Z_h = e^{ik_h\Delta x}. \tag{8}$$

In the discrete frequency domain this becomes

$$Z_h = e^{iq_h\Delta k_h\Delta x}, \tag{9}$$

where q_h is the integer frequency index that lies in the range, $0 \leq q_h < N_xN_y$. The uncertainty relationship, $\Delta k_h\Delta x = \frac{2\pi}{N_xN_y}$, allows this to be simplified still further, leaving

$$Z_h = e^{2\pi i\,\frac{q_h}{N_xN_y}}. \tag{10}$$

If we find a form of q_h in terms of Fourier indices, q_x and q_y, that can be plugged into equation (10) in order to satisfy equations (4) and (5), this will provide the link between k_h and spatial wavenumbers, k_x and k_y.

The idea that x-axis wavenumbers will have a higher frequency than y-axis wavenumbers, leads us to try a q_h of the form,

$$q_h = N_yq_x + q_y. \tag{11}$$

Substituting this into equation (10) leads to

$$Z_h \;=\; e^{2\pi i\,\frac{(N_yq_x+q_y)}{N_xN_y}} \tag{12}$$

$$= e^{2\pi i\left(\frac{q_x}{N_x}+\frac{q_y}{N_xN_y}\right)}. \tag{13}$$

Since q_y is bounded by N_y, for large N_x the second term in braces $\frac{q_y}{N_x N_y} \approx 0$, and this reduces to

$$Z_h \approx e^{2\pi i \frac{q_x}{N_x}} = Z_x, \tag{14}$$

which satisfies equation (4).

Substituting equation (11) into equation (10), and raising it to the power of N_x leads to:

$$Z_h^{N_x} = e^{2\pi i \frac{(N_y q_x + q_y)}{N_y}} \tag{15}$$

$$= e^{2\pi i \left(q_x + \frac{q_y}{N_y}\right)}. \tag{16}$$

Since q_x is an integer, $e^{2\pi i q_x} = 1$, and this reduces to

$$Z_h^{N_x} = e^{2\pi i \frac{q_y}{N_y}} = Z_y, \tag{17}$$

which satisfies equation (5).

Equation (11), therefore, provides the link we are looking for between q_x, q_y, and q_h. It is interesting to note that not only is there a one-to-one mapping between 1-D and 2-D Fourier components, but equation (11) describes helical boundaries in Fourier space: however, rather than wrapping around the x-axis as it does in physical space, the helix wraps around the k_y-axis in Fourier space (Figure 2). This provides the link that is missing in Figure 1, but shown in Figure 3.

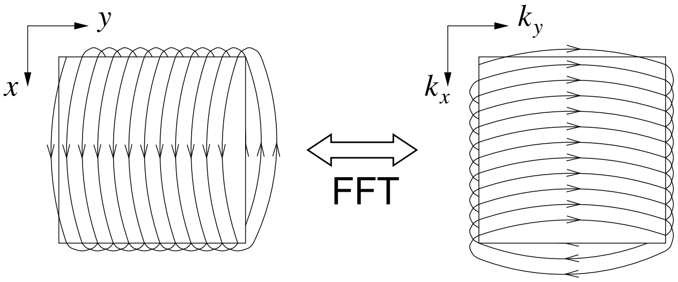

Figure 2: Fourier dual of helical boundary conditions is also helical boundary conditions with axis of helix transposed. james1-transp [NR]

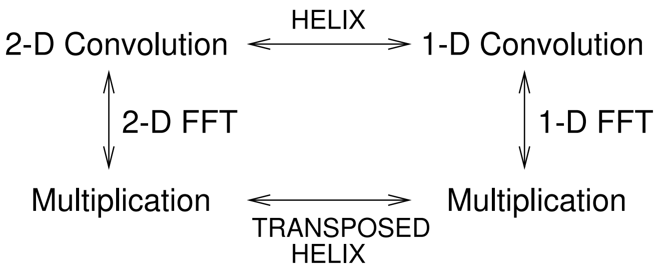

Figure 3: Relationship between 1-D and 2-D convolution, FFT's and the helix, illustrating the Fourier dual of helical boundary conditions. james1-ill2 [NR]

As with helical coordinates in physical space, equation (11) can easily be inverted to yield

$$k_x = \Delta k_x \, q_x = \frac{2\pi}{N_x \Delta x} \left[\frac{q_h}{N_y} \right], \qquad \text{and} \tag{18}$$

$$k_y = \Delta k_y \, q_y = \frac{2\pi}{N_y \Delta y} \left(q_h - N_y \left[\frac{q_h}{N_y} \right] \right) \tag{19}$$

where $[x]$ denotes the integer part of x.

Speed comparison

For a two-dimensional dataset with dimensions, $N_x \times N_y$, the cost of a 1-D FFT in helical coordinates is proportional to

$$N_x N_y \log\left(N_x N_y\right). \tag{20}$$

For the same dataset, the cost of a 2-D FFT is

$$\begin{aligned} N_y\left(N_x \log N_x\right) + N_x\left(N_y \log N_y\right) &= N_x N_y \left(\log N_x + \log N_y\right) \\ &= N_x N_y \log\left(N_x N_y\right). \end{aligned} \tag{21}$$

Therefore, the cost of a 1-D helical FFT of a 2-D dataset is exactly the same as the cost of an 2-D FFT of the same dataset. The link between the two leads to no computational advantages in the number of operations. However, other differences may lead to computational savings. For example, a 2-D FFT with a power-of-two algorithm requires both N_x and N_y to be powers of two. However, the 1-D helical FFT requires just $N_x N_y$ to be a power of two, and so less zero-padding may be required. The corollary, that a large 1-D FFT can be computed (with small inaccuracies) using a 2-D FFT algorithm, also leads to potential computational savings. Two-dimensional FFT's are easier to code to run both in parallel and out-of-core than 1-D FFT's, leading to significantly faster code and a lower memory requirement without the additional complexity of Singleton's algorithm (Press et al., 1992).

EXAMPLES

Figure 4 compares the real part of the 2-D Fourier transform of a single spike with the equivalent real part after a 1-D FFT in helical boundary conditions. The Fourier transforms are centered, so that zero frequency is at the center of the plot. This has the effect that the artifacts that would appear at the vertical boundaries ($k_y = 0$) of the image are more visible since they appear at the center of the plot.

Figure 5 compares amplitude spectra for a broader band 2-D seismic VSP gather. Artifacts from the helical boundaries are very difficult to see on the spectra themselves, and the difference image is very low amplitude.

Application to the multiple prediction

Multiple prediction is the first step in the class of adaptive multiple suppression methods (Verschuur et al., 1992). In a laterally homogeneous earth, Kelamis and Verschuur (2000) show that surface-related multiples can be predicted by taking the multi-dimensional auto-convolution of a common midpoint (CMP) gather. This auto-convolution reduces to a multiplication in the *f-k* domain, and so it can be performed rapidly with multi-dimensional FFT's.

Since multi-dimensional FFT's can be computed with a one-dimensional Fourier transform in helical coordinates, we can predict multiples by wrapping a CMP gather onto a helix, taking its 1-D FFT, squaring the result, and returning to the original domain.

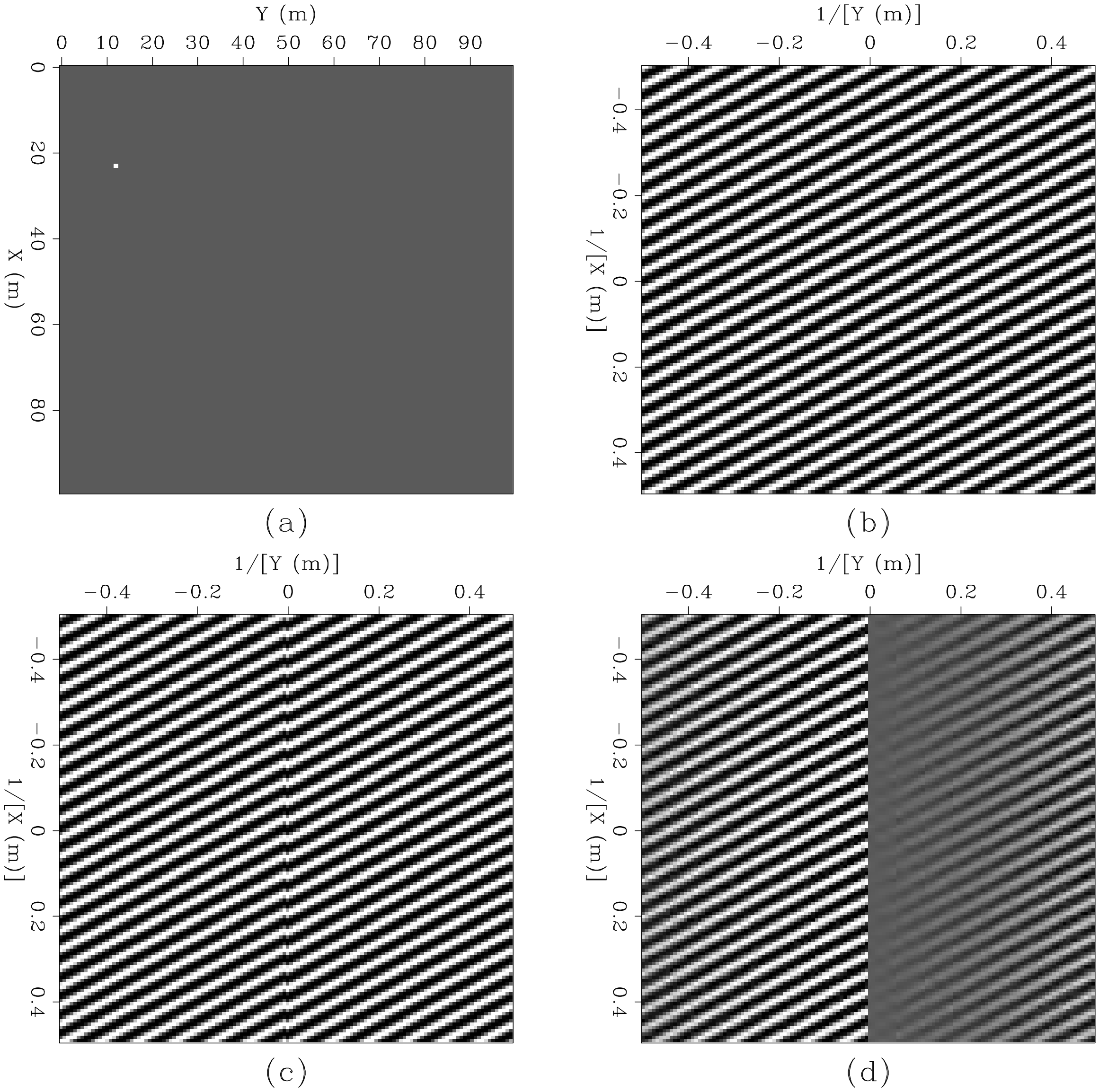

Figure 4: Comparison of real part of 2-D spectra: (a) input spike (single frequency), (b) real part of 2-D FFT, (c) real part of 1-D helical FFT, and (d) difference between (b) and (c) clipped to same level. james1-spikespec [ER,M]

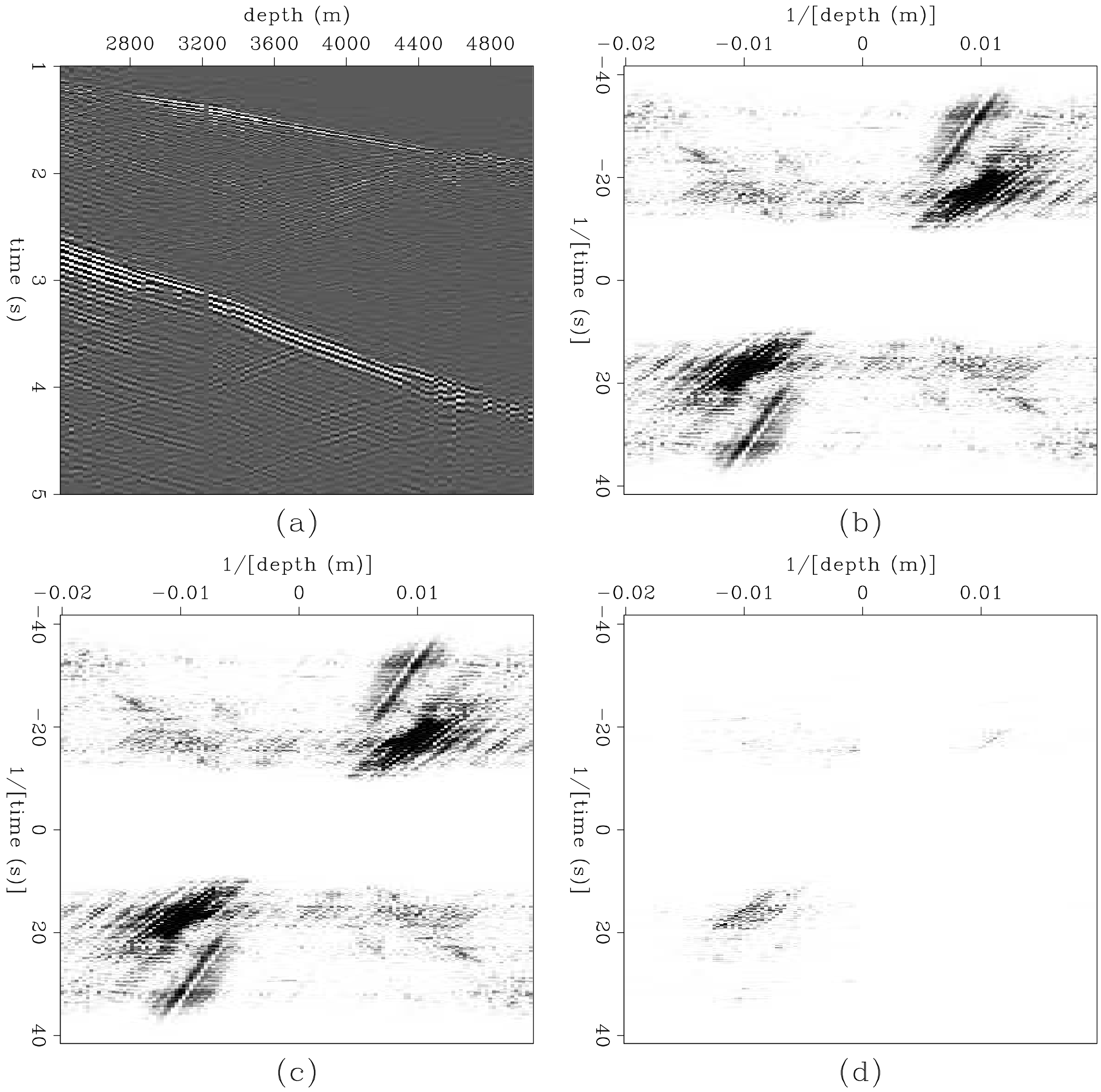

Figure 5: Comparison of 2-D amplitude spectra: (a) input 2-D VSP gather, (b) amplitude spectrum from 2-D FFT, (c) amplitude spectrum from 1-D helical FFT, and (d) difference between (b) and (c) clipped to same level. james1-schlumspec [ER,M]

We tested this algorithm on a single CMP from the synthetic BP multiple dataset (Clapp, 1999). Figure 6 displays the multiple prediction result using the helical coordinate system and only a single one-dimensional FFT. Theoretically, only first-order multiples should have correct relative amplitudes, and the source wavelet appears twice in the multiple prediction. However, the kinematics of all multiples are almost exact, even for higher-order multiples below 5 s two-way traveltime.

CONCLUSION

We have explicitly found the relationship between multi-dimensional FFT's and 1-D FFT's on a helix, linking the wavenumber vector, $\mathbf{k}$, in a multi-dimensional system with the wavenumber of a helical 1-D FFT, k_h. Specifically, the Fourier dual of helical boundary conditions is helical boundary conditions but with axes transposed. We have illustrated the concepts with an example of multi-dimensional multiple prediction.

REFERENCES

Claerbout, J. F., 1998a, Geophysical estimation by example: available on the World-Wide-Web at http://sepwww.stanford.edu/prof/gee/.

Claerbout, J. F., 1998b, Multidimensional recursive filters via a helix: Geophysics, **63**, 1532–1541.

Clapp, R. G., 1999, BP multiple synthetic: SEP Data Library.

Kelamis, P. G., and Verschuur, D. J., 2000, Surface-related multiple elimination on land seismic data-Strategies via case studies: Geophysics, **65**, no. 3, 719–734.

Press, W. H., Teukolsky, S. A., Vetterling, W. T., and Flannery, B. P., 1992, Numerical recipes: The art of scientific computing: Cambridge University Press, 2nd edition.

Verschuur, D. J., Berkhout, A. J., and Wapenaar, C. P. A., 1992, Adaptive surface-related multiple elimination: Geophysics, **57**, no. 9, 1166–1177.

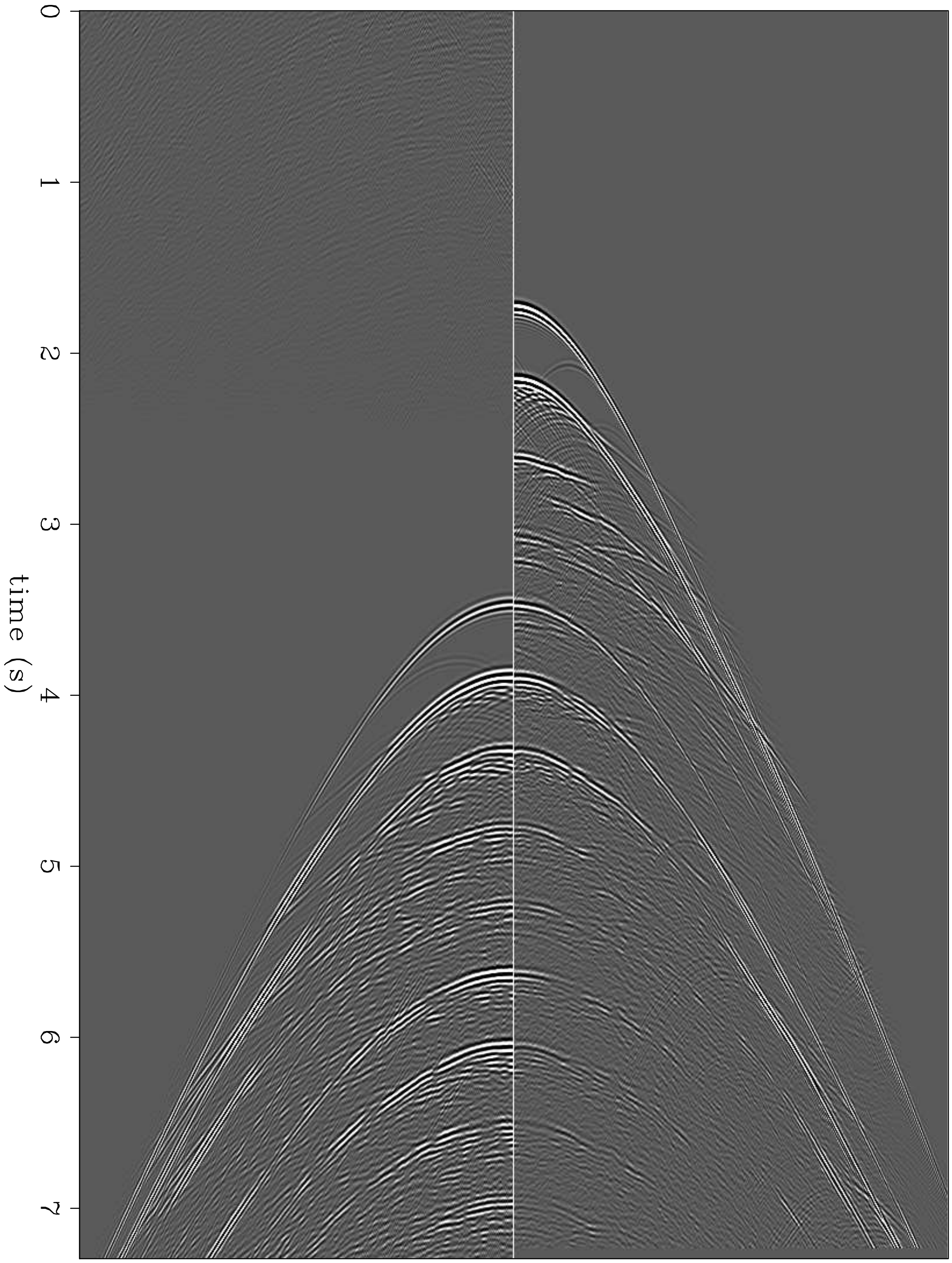

Figure 6: The left panel shows the multiple model obtained with the helix and a 1-D FFT. The right panel shows the input CMP gather with the offset axis reversed to facilitate the comparison. Some wrap-around effects appear at the top of the multiple model. james1-BP2 [ER]